Scripta Materialia 158 (2019) 6–10

Contents lists available at ScienceDirect

Scripta Materialia

journal homepage: www.elsevier.com/locate/scriptamat

The heterogeneous microstructure of heat affect zone and its effect on creep resistance for friction stir joints on 9Cr–1.5 W heat resistant steel

Chao Zhang, Lei Cui *, Dongpo Wang, Yongchang Liu, Chenxi Liu, Huijun Li

Tianjin Key Laboratory of Advanced Joining Technology, School of Materials Science and Engineering, Tianjin University, Tianjin 300354, PR China

ARTICLE INFO

Article history:
Received 9 July 2018
Received in revised form 14 August 2018
Accepted 15 August 2018
Available online xxxx

Keywords:
Friction stir welding
Heat resistant steel
Heat affect zone
Heterogeneous microstructure
Creep resistance

ABSTRACT

The heterogeneity of microstructures in heat affect zone of 9Cr-1.5 W heat resistant steel friction stir welding joint was studied, and its influence on the weld creep property was discussed. The inter critical heat affect zone at the advancing side of the weld is found as the most likely area to be failure during creep, owing to the formation of ferrite grains and lath martensite with low carbon content and the coarsening of $M_{23}C_6$ carbides. The as-welded joint exhibits a good creep resistance of 1173.8 h creep rupture time at 600 °C temperature and 200 MPa stress.

© 2018 Acta Materialia Inc. Published by Elsevier Ltd. All rights reserved.

Reduced activation ferritic/martensitic (RAFM) steel contains 9%Cr and alloyed with low activation elements of W and Ta, is a candidate structure material for the first wall and blanket in nuclear reactors [1–3]. To fusion welding of RAFM and similar steels, the heterogeneous microstructure of heat affect zone (HAZ) has detrimental effect on the creep properties of the weldment, which means lower creep strength and shorter rupture time than that of the base material, a key in-service problem of RFAM steel weldment [4,5]. In fusion welds, there are critical zones involved in HAZ, known as fine grain heat affect zone (FG-HAZ) and inter critical heat affect zone (IC-HAZ), formed in a welding thermal cycle by heating to A_{C1}~A_{C3} and above A_{C3} of the steel, respectively [6,7]. In FG-HAZ and IC-HAZ, the time for the dissolution of carbides and diffusion of carbon atoms into the austenite is highly limited owing to the extremely high cooling rate during welding [8]. Therefore, the austenite formed in FG-HAZ has a low carbon content, and the martensite transformed will also have a low carbon content, with an associated low hardness and creep strength [9,10].

Friction stir welding (FSW) is now receiving more attractive to be used in welding RAFM steels [11,12]. In FSW, the welding peak temperature might be lower than the A_{C3} point or even A_{C1} of the steel by decreasing the ratio of rotational speed and traverse speed [13,14]. Therefore, a better creep property of heat resistant steel joint could be desired when using FSW. However, it is still a question that whether high creep resistance of FSW RAFM joint can be achieved. The understanding of the relationships between the microstructure and creep property in FSW joint is still a scarcity. Here we reported are concerning on the creep rupture behavior of FSW joint for 9% Cr RAFM steel and its relationship to the weld microstructures.

Several 5 mm thick RFAM steel plates were used as the base material. The chemical composition is 8.8% Cr, 1.5% W, 0.1% C, 0.46% Mn, 0.2% V, 0.083% Ta, 0.087% Si and 0.013% N (wt%). The A_1 and A_3 temperature of the steel are 881 °C and 956 °C, and the complete dissolution temperature of $M_{23}C_6$ phase is 896 °C. The welding tool is made of W-25% Re alloy and contains an 18 mm diameter concave shoulder and a 4.7 mm length tapered probe with screw threads. Rotational speeds of 200 rpm, 300 rpm and 400 rpm and a unique traverse speed of 60 mm/min were employed for FSW. The axial force and tilt angle were 10 kN and 2.5°. Creep tests were conducted at 600 °C and 650 °C and creep stress of 200 MPa. According to ASTM E139-2006, the creep specimens were machined perpendicular to the weld seam with a gauge length of 20 mm and cross-sectional area of 6 × 2.5 mm. Zeiss Auriga Focused Ion beam system was used to cut IC-HAZ and FG-HAZ samples from the weld. A OLYMPUS GX51 optical microscope (OM), JEOL-7800 scanning electron microscope (SEM) with an electron back scatter diffraction (EBSD) module, and Tecnai G2F30 transmission electron microscope (TEM) were used to examine the microstructures of the weld regions where interested.

The creep curves of the joints and BM are shown in Fig. 1a & b. At 650 °C/200 MPa, the creep rupture time (ranged in 5.134–7.521 h) and steady creep stage of the FSW joints are shorter than that of BM (17.8 h). At 600 °C/200 MPa, the creep rupture time of BM is 3398 h, while the FSW joints welded with 200 rpm and 400 rpm rotational speeds are decreased to 1173.8 h and 858.29 h, respectively. Clearly, the rupture time of FSW RAFM steel joint obtained at 600 °C/200 MPa is longer than that of TIG joint obtained at 550 °C/180 MPa [15]. It

* Corresponding author.
E-mail address: leicui@tju.edu.cn (L. Cui).

https://doi.org/10.1016/j.scriptamat.2018.08.028
1359-6462/© 2018 Acta Materialia Inc. Published by Elsevier Ltd. All rights reserved.

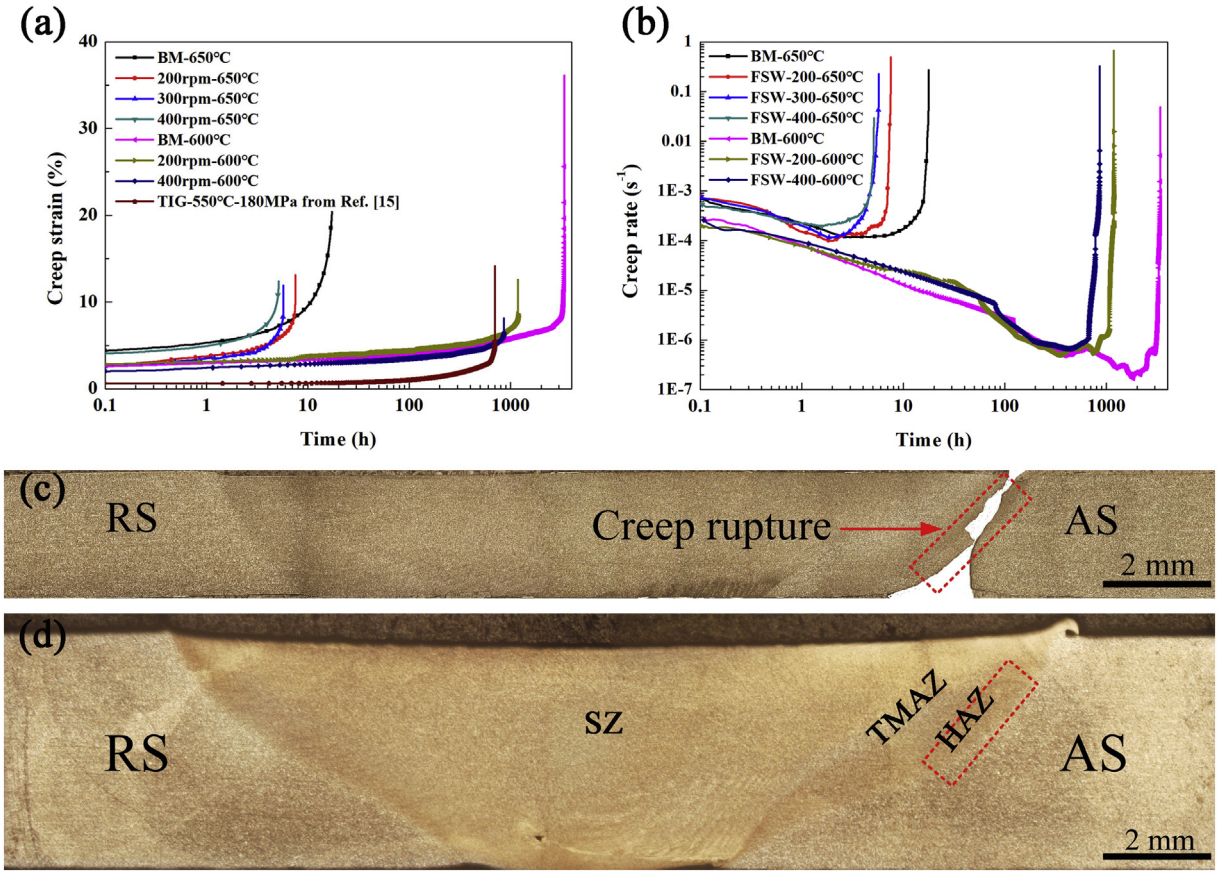

Fig. 1. (a) and (b) are the creep curves showing the creep strain and creep rate versus to the creep time, (c) the rupture specimen and (d) the cross-section of the joint welded the 200 rpm rotational speed.

reveals that much higher creep resistance of the joint for RAFM steel can be achieved by FSW than that by TIG. As the FSW rotational speed is increased from 200 rpm to 400 rpm, the creep rupture time of the joint can be decreased, showing that the creep resistant of FSW RAFM joint is sensitive to the welding heat input and is in direct proportion to the ratio of rotational speed and traverse speed or welding heat input.

During creep tests, all the creep specimens are fractured at the edge of HAZ at the advancing side of the weld (AS-HAZ), a transition region between HAZ and BM which is characterized by partially austenitic recrystallization and martensitic transformation. By observing the microstructure of AS-HAZ, as shown in Fig. 2a & b, the creep rupture region is confirmed as the IC-HAZ between FG-HAZ and BM. The definition of IC-HAZ and FG-HAZ is accordance with the gradient microstructural variation caused by the gradient temperature field throughout the weld. As shown in Fig. 2c–f, in IC-HAZ, a part of tempered martensite is austenitized and then transformed to lath martensite, and in FG-HAZ the tempered martensite is fully austenitized and then transformed to lath martensite. Owing to the high cooling rate of FSW, the grain growth in IC-HAZ and FG-HAZ can be restrained. Therefore, the above two regions are characterized by significant grain refinement [16,17].

It can be found from Fig. 2 that the microstructure of AS-HAZ is heterogeneous, particularly in the grain structures and grain sizes, and such heterogeneity of AS-HAZ could be enhanced with increasing the rotational speed. The other two regions are found as stir zone (SZ) and thermal mechanically affect zone (TMAZ) which are commonly formed in FSW steel joint. The EBSD mapping results (Fig. 2g–i.) reveal that the average grain sizes for BM, IC-HAZ, and FG-HAZ are 5.64 μm, 4.02 μm, and 3.39 μm, respectively. The fractions of high angle grain boundaries (HABs) in IC-HAZ and FG-HAZ are 43.8%, and 47.6%, which are lower than BM of 50.5%. One key reason for the reduction of HABs in HAZ is the locally heating and cooling cycles in FSW, which generates unmatched thermal expansion and contraction forces, leading to complicated thermal stress and the change of microstructure [18].

The TEM images for the microstructures in BM, IC-HAZ, FG-HAZ and TMAZ of the joint welded with 400 rpm are shown in Fig. 3a–d, respectively. To confirm the types of precipitations within the material, the selected area electron diffraction (SAED) results revealing the lattice parameters are shown in Fig. 3e&f. As shown Fig. 3a, the BM microstructure is mainly of tempered martensite and contains $M_{23}C_6$ precipitate particles at prior austenite grain boundaries and martensite lath boundaries. Within the tempered martensite, several nano-sized MX particles are observed. The number density and average size of these particles were calculated through TEM observations to be 6.52×10^{10} m^{-2} and 85 ± 3 nm for $M_{23}C_6$ phase, 1.18×10^{11} m^{-2} and 20 ± 2 nm for MX particles.

As shown in Fig. 3b, the IC-HAZ, both tempered martensite and lathy martensite could be observed. The diameter of spherical $M_{23}C_6$ carbides in IC-HAZ is around 100 nm with a number density of 4.86×10^{10} m^{-2}. The diameter and number density of MX phases in IC-HAZ are 25 ± 1 nm and 1.06×10^{11} m^{-2}, respectively. In FG-HAZ, as shown in Fig. 3c, a nearly full lath martensite microstructure containing a high density of dislocations is obtained. The precipitates detected in FG-HAZ are $M_{23}C_6$ with size of 73 ± 3 nm and number density of 3.32×10^{10} m^{-2} and MX with size of 15 ± 1 nm and number density of 1.15×10^{11} m^{-2} at martensite lath boundaries and dislocations within martensite laths, respectively. In TMAZ, as revealed in Fig. 3d, a full lath martensite microstructure involving finer but fewer $M_{23}C_6$ precipitate particles than that in BM, IC-HAZ and FG-HAZ is observed. The spherical MX precipitate in TMAZ has a mean particle size of 12 ± 1 nm with a number density of 1.32×10^{11} m^{-2}, which is finer

Download English Version:

https://daneshyari.com/en/article/8943172

Download Persian Version:

https://daneshyari.com/article/8943172

Daneshyari.com